RSC Advances

PAPER

View Article Online
View Journal | View Issue

Cite this: *RSC Adv.*, 2025, **15**, 41899

Unveiling the adsorptive potential of *Populus ciliata* leaf powder for methylene blue removal from environmental samples

Salma Gul,[a] Nadeem Raza,[b] Maria Naseer,[c] Khalid Aziz,*[d] Hajera Gul,[e] Aaliya Minhaz,[e] Mohamed Khairy[b] and Abdelmonaim Azzouz[f]

Received 3rd September 2025
Accepted 20th October 2025

DOI: 10.1039/d5ra06607g

rsc.li/rsc-advances

To cope with environmental hazards caused by synthetic dyes, herein, we report an inexpensive biosorbent based on *Populus ciliata* leaf powder for the adsorption of methylene blue (MB) from aqueous solutions. Using FTIR, BET, EDX, and SEM, chemical, structural, and morphological characteristics of the biosorbent were examined. The batch adsorption experiments were performed to investigate the influence of contact time, pH, adsorbent dose, nature of water samples, and dye concentration for MB adsorption. At optimum conditions, maximum adsorption of 87.7% and adsorption capacity value of 21.21 mg g^{-1} was achieved at pH 7 for MB concentration of 10 mg L^{-1}. Langmuir and Freundlich isotherm models were applied to the equilibrium adsorption data, and the data were perfectly fitted to Langmuir isotherm model. Pseudo-first-order and pseudo-second-order (PSO) kinetic models were evaluated and it was found that the PSO was best fitted to the experimental data. MB was successfully adsorbed from environmental samples using the suggested biosorbent. This research can provide a viable approach to mitigating the health risks associated with dye pollution, thereby contributing to the reduction of environmental contamination.

1. Introduction

In light of the accelerated pace of industrialization, a wide range of contaminants including both organic and inorganic persistent toxic substances are being released into the natural environment at unprecedented levels.[1] Industrial runoff containing various pollutants such as dyes, pesticides, personal care, and pharmaceutical waste products is often discharged into freshwater sources without adequate treatment, posing serious risks to both aquatic ecosystems and human health.[2] Synthetic dyes are extensively used in a variety of industries, including paper, textiles, food, cosmetics, leather, plastics, and pharmaceuticals.[3] These industries frequently release substantial quantities of synthetic dyes into their effluents. Globally, approximately 700 000 tonnes of synthetic dyes are produced annually, of which more than 15% is directly discharged into aquatic environments.[4]

Methylene blue (MB) is one of the most prevalent synthetic dyes widely used as an indicator, a textile coloring agent, and in various other industrial applications.[5] Its extensive use makes it one of the most frequently detected dyes in aquatic environments. If not properly managed, MB can degrade the visual quality of water bodies and reduce their suitability for multiple uses. Contaminated water containing MB is harmful, xenobiotic, and potentially carcinogenic, underscoring the need for effective treatment of dye-containing effluents to mitigate their environmental impact.[6]

Dyes possess complex molecular structures that contribute to their physicochemical, optical, and thermal stability. These properties make them highly resistant to degradation by chemicals, heat, oxidizing agents, and microbial enzymes. Consequently, their release into the environment poses serious ecotoxicological threats. The primary techniques for dyes removal from wastewater fall into three categories: physical, chemical, and biological methods. However, highly soluble dyes are difficult to remove using simple physical methods, while chemical coagulation and flocculation, as well as biological processes, often prove ineffective in continuous operations.[7] To address these challenges, advanced techniques such as ozone treatment, ion exchange, membrane separation, electrochemical degradation, precipitation, and adsorption are widely employed. Among these, adsorption is regarded as one of the most cost-effective and selective treatment methods for water remediation.[8] Commercial activated carbon is the most

[a]*National Center of Excellence in Physical Chemistry, University of Peshawar, Pakistan*
[b]*Department of Chemistry, College of Science, Imam Mohammad Ibn Saud Islamic University (IMSIU), Riyadh, Saudi Arabia*
[c]*Department of Chemistry, Women University Swabi, KPK, Pakistan*
[d]*Institute of Chemical Sciences, Bahauddin Zakariya University Multan, Pakistan. E-mail: malikwains786@gmail.com*
[e]*Department of Chemistry, Shaheed Benazir Bhutto Women University, Peshawar, Pakistan*
[f]*Laboratory of Water, Research, and Environmental Analysis, Faculty of Sciences, Abdelmalek Essaadi University, Tetouan, Morocco*

commonly used adsorbent due to its high porosity and large surface area; however, its high-cost limits its large-scale applications compared to naturally occurring biosorbents. Additionally, utilization of biosorbents offers an economical and environment friendly alternative for dye removal, making it an increasingly popular choice in wastewater treatment.[9]

The selection of an adsorbent is tricky, as synthetic alternatives such as silica gel have excellent adsorption capacity; however, they are restricted by economics and regenerative concerns. The emphasis has turned to natural resources and waste products as affordable alternatives.[10] Natural organic waste such as peelings of fruits,[11] sawdust,[12] and nutshells[13] has been identified as an excellent adsorbent for different pollutants.[14] Plant-based materials high in lignin, cellulose, and other fibers function as active adsorption sites, with cellulose being the most common.[15] These components are easily accessible and typically demand no preliminary treatment, lowering costs and removing any requirement for rejuvenation.[16]

The leaf powder extracted from *Populus ciliata* (PC), commonly referred to as Himalayan poplar tree, has enormous prospects as a renewable and affordable biosorbent for the elimination of synthetic dyes like MB from water-based solutions. This efficiency is due to the plant's rich phytochemical content, which comprises tannins, flavonoids, cellulose, and several other polyphenolic chemicals that provide a range of functional groups on the surface of the adsorbent material, including hydroxyl (–OH), carboxyl (–COOH), and phenolic groups.[17] Various physical and chemical interactions including electrostatic attraction, hydrogen bonding, and π–π interactions, enable robust affinities between the adsorbent and cationic MB dye. PC leaf powder, a renewable and accessible biomass can provide an ecologically conscious and cost-effective substitute to traditional biosorbents, promoting ecological wastewater management solutions.[18]

A literature survey revealed that considering the plentiful supply and low cost, PC leaves have not been exploited as a biosorbent for adsorbing toxic dyes from wastewater. *Populus ciliata* proliferates in Pakistan's northern areas. Thus, the primary objectives of these laboratory-based batch adsorption investigations conducted with wastewater are: (a) to select and evaluate PC leaf biomass as a biosorbent for the adsorption of MB in aqueous solutions; (b) to establish the fundamentally critical process variables and their optimal levels affecting dye adsorption kinetics and equilibrium adsorption characteristics; and (c) to determine the strength, regeneration capacity, and adsorption performance of the biosorbent. The viability of PC leaf powder as an effective, economical, and sustainable source for MB dye adsorption from water sources was validated by adsorption results supported by a number of parameters, including temperature, time, pH, ionic strength, biosorbent amount optimization, dye concentration, and biosorbent reusability.

2. Materials and methods

2.1. Materials

In this work, the biosorbent used was *Populus ciliata* leaf powder, while the adsorbate was MB, obtained from Sigma (BDH, England). HCl (37%), ethanol, NaOH (99%), deionized water, NaCl (99%), KCl (99%), and $CaCl_2$ (98%), were obtained from Merck, Germany. All materials were employed without additional purification.

2.2. Equipment

A scanning electron microscope (JEOL, JSM-IT-100, Japan) was used to study the surface structure of the biosorbent before and after MB adsorption. Elemental analysis was performed using EDX at 20.00 kV electron acceleration voltage before and after MB adsorption onto the PC biosorbent. The FTIR spectrophotometer (Cary-630 Agilent Technologies USA) was used to analyze the functional groups present on the surface of the biosorbent (PC). The adsorbent's FTIR spectra were recorded in the 400–4000 cm^{-1} range. The specific surface area and pore volume of the biosorbent was determined using Autosorb iQ Station 2 (Anton Paar, United States). A digital orbital shaker (a product of PCSIR, Pakistan) was set at 200 rpm and operated at room temperature to ensure proper mixing of biosorbent and dye. The UV-visible spectrophotometer (Shimadzu, UV-3000, with a 1 cm path length) was used to measure absorbance of dye solutions.

2.3. Preparation of PC adsorbent

To synthesize *Populus ciliata* (Himalayan poplar) leaf powder, fresh leaves of PC plants from the Swabi village area in Pakistan's KPK province were collected. To remove dust and other pollutants, the PC leaves were carefully cleaned and repeatedly rinsed with water. The materials were shaded-dried for 96 h before being ground into fine powder.

3. Result and discussion

3.1. Characterization

3.1.1. FTIR analysis. The FTIR spectra (Fig. 1) of the biosorbent (PC) presented multiple distinct and strong peaks at 460, 570, 1032, 1450, 1531, 1602, 1729, 2914 cm^{-1}, and 3280 cm^{-1}. The peak around 460 cm^{-1} was assigned to C–H bending vibrations. Polysaccharides like cellulose and hemicellulose exhibit C–H stretching and C–O–C out-of-plane stretching vibrations, resulting in the band at 570 cm^{-1}. The bands at 1032 cm^{-1} and 1602 cm^{-1} represent C–O and N–H bending, respectively. The presence of these bands indicates specific chemical groups in the biosorbent material. Moreover, the bending and stretching vibrations of $–CH_2$ in cellulose, as well as the –C–O vibrations in hemicellulose and cellulose, can be correlated with the peaks at 1032 cm^{-1} and 1602 cm^{-1} (strong band). The 1450 cm^{-1} peak corresponds to C–H bending vibrations of aliphatic groups ($–CH_2$ and $–CH_3$) and asymmetrical bending of methyl groups found in FTIR spectrum. This band represents the bio polymer framework of the PC leaves. Prominent peak at 1531 cm^{-1} represents N–H bending (amide II band) and C=C stretching vibrations of aromatic rings, indicating the possible existence of proteins, and other aromatic chemicals. This implies that phenolic and nitrogenous components may have a role in possible adsorption

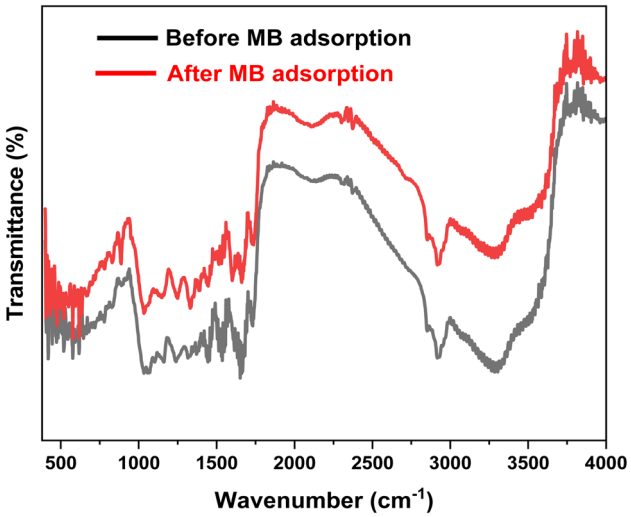

Fig. 1 FTIR spectra of *Populus ciliata* leaf powder.

interactions with contaminants. Another peak at 1729 cm^{-1} (medium intensity) indicates C=O stretching of carboxylic acid with intramolecular hydrogen bonding. This peak is associated with ionized non-coordinated and coordinated COO^- groups. The peak around 2914 cm^{-1} was attributed to symmetric and asymmetric C–H stretching of aliphatic acids. Broad peak around 3280 cm^{-1} was attributed to the presence of hydroxyl radicals. The presence of functional groups such as –OH, –COOH, and –C=O is crucial for the adsorption process, as they provide sites for interaction with dyes. FTIR analysis confirms that powdered PC contains these functional groups. The adsorbent's structural reliability was confirmed by the comparable prominent peaks in the PC leaf powder FTIR spectrum after the MB adsorption. However, a substantial decrease in peak intensities after MB adsorption suggests that surface functional groups-such as hydroxyl, carboxyl, carbonyl, and amide moieties are actively involved in MB binding. The lowering in peak intensities may occur due to various types of electrostatic interactions including hydrogen bonding and π–π

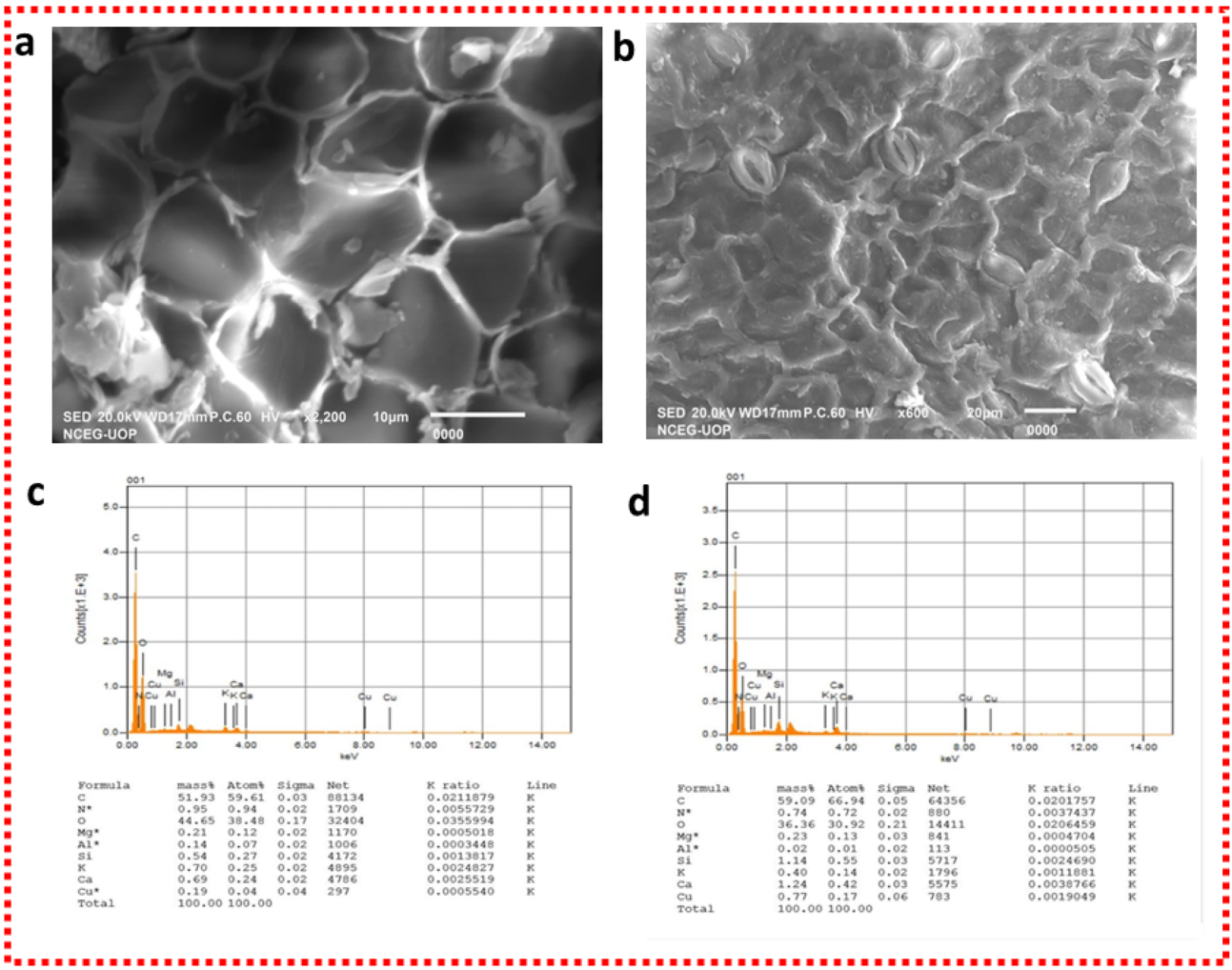

Fig. 2 SEM image of *Populus ciliata* leaf powder before adsorption (a), after adsorption of MB (b), EDX image of *Populus ciliata* leaf powder before adsorption (c), after adsorption of MB (d).

interactions with MB molecules, exhibiting successful surface adsorption without significantly altering the biosorbent surface.[19,20]

3.1.2. Scanning electron microscopy and energy dispersive X-ray. Scanning electron microscopy was used to investigate the morphological properties of the biosorbent. SEM analysis (Fig. 2(a and b)) revealed a significant difference in the surface of the PC biosorbent before and after MB dye adsorption. The SEM image of PC leaf powder (Fig. 2a) presented a surface with distinctive characteristics, characterized by its rough, porous, and uneven texture. These surface features offered promising sites for effective dye adsorption. The inherent roughness and surface porosity establish PC leaf powder as a proficient biosorbent for dye adsorption. Subsequent to the adsorption process, the surface of PC leaf powder (Fig. 2b) demonstrated surface transformation as it became covered with MB, resulting in a smoother texture attributed to the entrapment of dye molecules.

The compositional behavior of the biosorbent was investigated using EDX spectroscopy to determine its elemental composition. The biosorbent exhibited the highest percentage of carbon and oxygen, as well as small amounts of nutrients as evident in the EDX spectra (Fig. 2(c and d)). The presence of more than 95% by weight of carbon and oxygen before and after MB adsorption confirmed the abundance of organic functional moieties in PC leaf powder. EDX spectra also indicated the presence of multiple natural mineral components (around 5%) on the adsorbent's surface before and after the adsorption of MB, including N, Mg, Si, Al, Cu, K, and Ca. Slight fluctuations in the weight percentages of carbon and oxygen before and after MB adsorption may signify the adsorption of MB.[21,22]

3.1.3. BET analysis. The Brunauer–Emmett–Teller (BET) study, which used the Langmuir adsorption model, revealed satisfactory linearity within the specified relative pressure range (0.05–0.3). *Populus ciliata* leaf powder possessed an estimated specific surface area of 4.454 $m^2\ g^{-1}$. The modest surface area indicates the PC leaf powder's porous and textured composition which combined with a number of surface functional groups (–OH, –COOH, –NH) allows to achieve successful MB adsorption *via* electrostatic attraction and hydrogen bonding instead of focusing on just its surface area. Thus, despite having a relatively modest BET surface area, PC leaf powder exhibits excellent adsorption capability, indicating that chemical activity and surface energies are more important than overall surface area in the removal of MB.

The t-plot was used to separate microporous and exterior surface regions of PC leaf powder (Fig. 3). The study produced a high correlation coefficient ($r = 0.9957$), suggesting that the data was linear and reliable. The micropore volume (0.006 $cm^3\ g^{-1}$) and area (12.711 $m^2\ g^{-1}$) indicate a moderate quantity of micropores inside the adsorbent structure. The adsorbent's exterior surface area (9.449 $m^2\ g^{-1}$) indicates that it is mostly microporous, with little or no involvement from mesopores or macropores. External surface area may be calculated by extrapolating the t-plot line when the surface area is nearly completely attributable to micropores, indicating high nitrogen adsorption at small relative pressures.

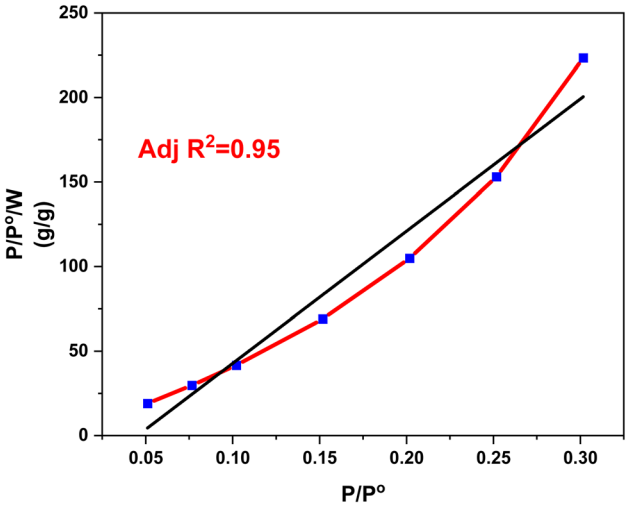

Fig. 3 t-Plot for pore volume investigations.

The N_2 adsorption–desorption examination of PC leaf powder indicated a total pore volume of $1.676 \times 10^{-3}\ cm^3\ g^{-1}$ for pores smaller than 2.6 nm at a relative pressure (P/P_0) of 0.30167. The predominance of pores in this region suggests the existence of microporous structures, which give a substantial amount of adsorption sites for adsorbate (MB). The tiny pore width promotes surface–solute associations through enabling MB to make intimate contact with the adsorbent's interior surface. This microporous structure contributes considerably to the excellent adsorption capacity and quick diffusion of MB molecules into the pore network, proving PC leaf powder's applicability as an effective adsorbent for MB adsorption.[23,24]

3.2. Effect of various parameters on MB adsorption

3.2.1. Effect of biosorbent dosage on MB adsorption. The impact of biosorbent dose on the MB adsorption was investigated by varying biosorbent doses ranging from 10 mg to 100 mg (Fig. 4(a)). The results revealed that the percentage adsorption of the MB dye increased with an increase in biosorbent dosage, reaching maximum at biosorbent dose of 60 mg. Beyond a biosorbent dosage of 60 mg, there was a slight decrease in MB adsorption. The increase in adsorbent dosage up to 60 mg provides sufficient active sites for the adsorption of dye onto PC leaf powder. However, when the biosorbent dosage increased from 60 mg to 100 mg, a slight decrease in MB adsorption was observed, which may be due to solution opacity and less trapping of active species due to agglomeration of biosorbents particles.[25] Thus, the optimal dosage for the adsorption of MB was taken as 60 mg for further experiments.

3.2.2. Effect of MB concentration on MB adsorption. To investigate the effect of initial MB concentration on the adsorption process, MB concentration was tested for different solutions (10 mg L^{-1} to 100 mg L^{-1}) (Fig. 4(b)). It was noted that with increasing dye concentration, a decrease in MB adsorption was observed. When the dye concentration was increased from 10 to 100 mg L^{-1}, the percent adsorption efficiency decreased from 87.7% to 57%. This decrease is understandable as a fixed

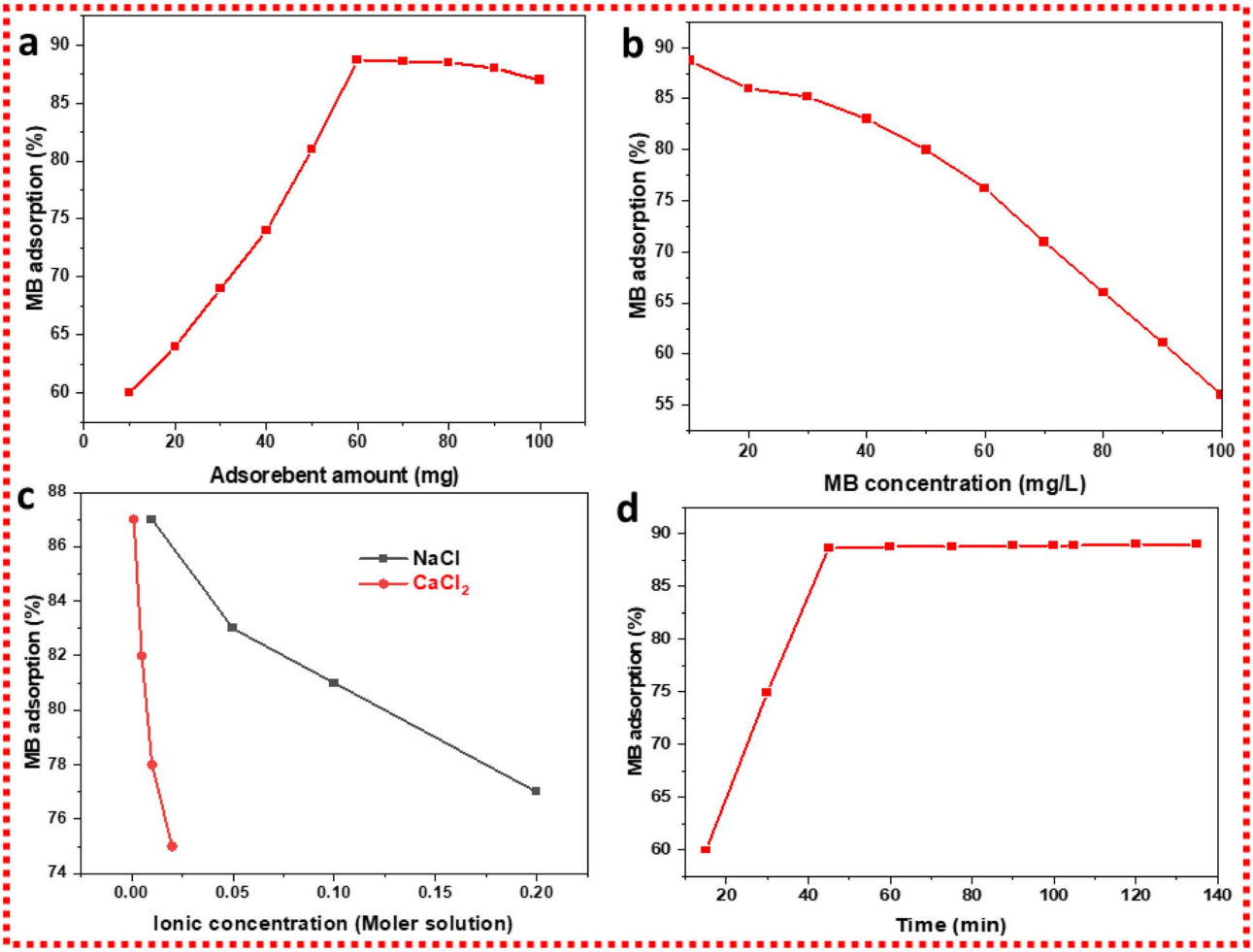

Fig. 4 Effect of biosorbent dose on MB adsorption (a), effect of MB concentration on MB adsorption (b), ionic strength effect on MB adsorption (c), effect of contact time on MB adsorption (d).

amount of biosorbent provides a specific number of active sites for adsorbate particles while additional sites are required for adsorption with increasing dye concentration. Hence, 10 mg L^{-1} was chosen as optimum MB concentration for MB adsorption investigations.[26]

3.2.3. Effect of ionic strength on MB adsorption. Dye effluents contain a mixture of ions that can interact and potentially affect the adsorption process of adsorbates on adsorbent surfaces. Significant amounts of salts are generally found in industrial and real-world water samples, and these salts may compete with target dyes for the active sites on adsorbent surfaces. Consequently, it is valuable to investigate the effect of ionic strength on the adsorption of MB using PC leaf powder (Fig. 4(c)). For this purpose, two common ionic species, NaCl and $CaCl_2$, were used to investigate the effect of ionic strength on MB adsorption. The presence of NaCl and $CaCl_2$ in solution affected the overall MB adsorption on biosorbents surface. It was observed that the percentage adsorption efficiency of MB decreased as the salt concentration increased. Since $CaCl_2$ produced more ions compared to NaCl, it was noted that more profonde effect was observed in case of $CaCl_2$.[19] This decrease in MB adsorption efficiency could be attributed to the competition between dye ions and competing ions such as Na^+, Ca^{2+}, and Cl^- ions for available sorption sites.[27]

3.2.4. Effect of contact time on MB adsorption. Contact time is crucial for the sorption process as it significantly affects adsorption process and determines the equilibrium time. During the initial stages, there was a rapid increase in the amount of MB adsorbed onto the biosorbent due to the abundance of available porous active sites on the biosorbent's surface (Fig. 4(d)). It was noted that MB adsorption was rapid initially, as maximum MB molecules were available for adsorption. Further, equilibrium between adsorbate and biosorbent was achieved in 45 minutes, following equilibrium, no appreciable change in MB adsorption was observed. Consequently, a contact time of 45 min was identified as the optimal duration for the adsorption of 10 mg per L MB using 60 mg dose of PC leaf powder as the biosorbent.[28]

3.2.5. Point of zero charge calculation and effect of pH on MB adsorption. Point of zero charge (PZC) relates to the pH at which surface of adsorbent behaves neutral. PZC of PC leaf

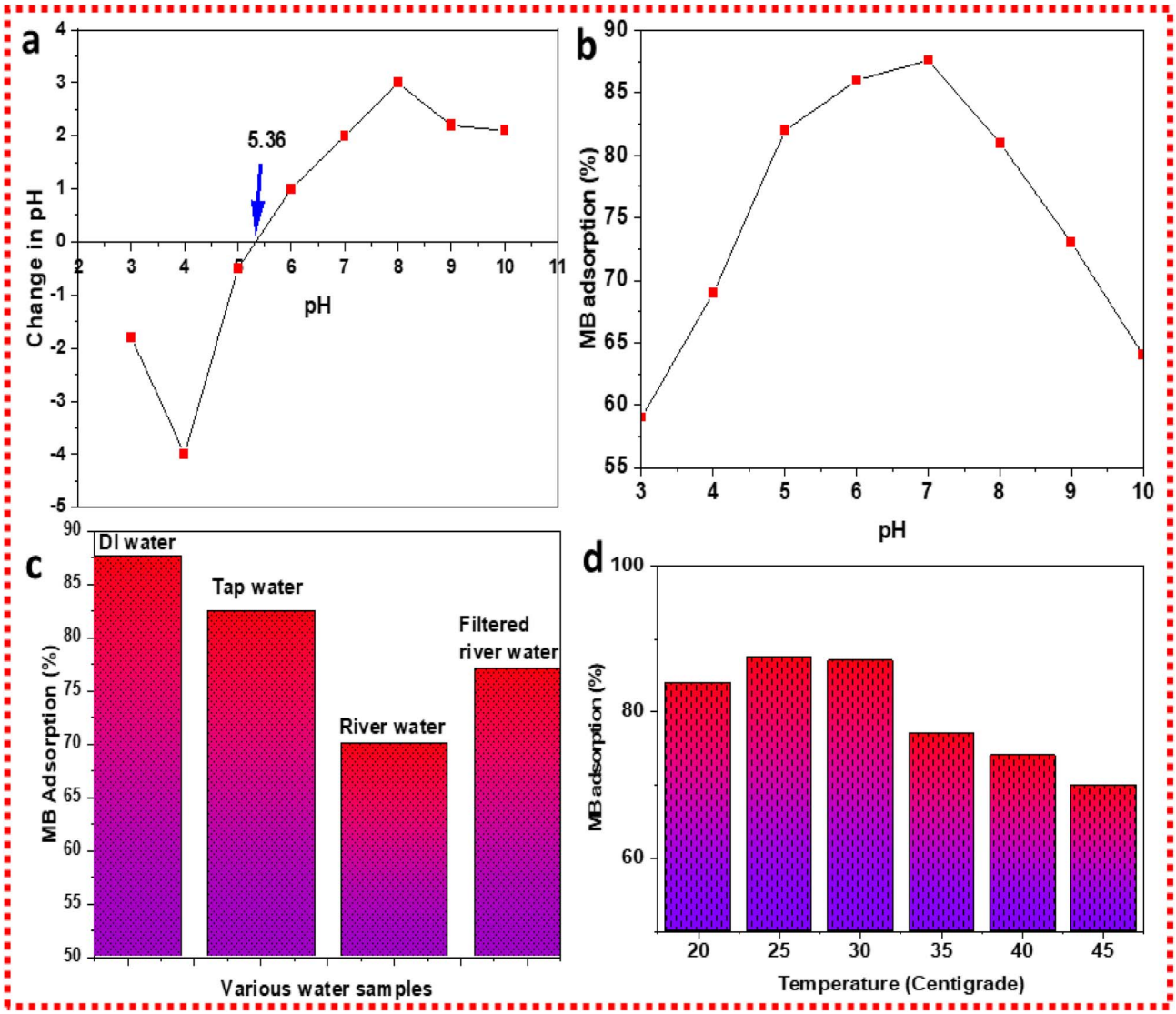

Fig. 5 PZC of PC leaf powder (a), pH effect on MB adsorption (b), effect of various water sources on MB adsorption (c), effect of temperature on MB adsorption (d).

powder was around 5.36 (Fig. 5(a)). Above this pH, the surface of the biosorbent is negatively charged, while below this pH, the biosorbent's surface acts as positively charged.

pH investigations for MB adsorption using PC leaf powder were performed at different pH values from 2–10 (Fig. 5(b)). MB is a cationic dye which behaves as positive in acidic conditions and negative in basic conditions. It was observed that maximum adsorption of MB using the biosorbent was achieved at neutral pH due to maximum interaction of MB with biosorbent. In acidic conditions, as elaborated by the PZC, the biosorbent shows positive character and MB also shows positive character; hence, interactions are minimum. Similarly, in basic conditions, both MB and the biosorbent show negative character, resulting in least interactions.[29,30,31]

3.2.6. Effect of different water resources on MB adsorption. To investigate the performance of the biosorbent for practical use in real water samples, its adsorption efficiency was also evaluated using water collected from different sources, such as distilled water (DI) water, tap water, river water, and filtered river water. The findings indicate that the percentage of dye adsorbed in various water samples was 87.7% in distilled water, 82.5% in tap water, 70% in river water, and 77% in filtered river (Fig. 5(c)). Least MB adsorption among various sources in river water was due to higher content of impurities and ionic species present in river water.[32] This demonstrates that the prepared biosorbent is practically effective in treating wastewater, and the biosorbent performed exceptionally well in real water samples. It can be concluded that this biosorbent can be used to effectively adsorb contaminants from real world water samples.[32]

3.2.7. Effect of temperature on MB adsorption. The adsorption mechanism is considerably temperature dependent, since the binding capability of a conventional adsorbent for an individual pollutant varies with the temperature of the reaction medium. A sequence of investigations was performed to study the influence of temperature on the adsorption of MB on PC leaf

powder. The medium temperature was varied from 20–45 °C while maintaining the remaining variables constant (MB: 10 mg L^{-1}, biosorbent dosage: 60 mg, pH of solution: 7, and sorption contact time: 45 min). As indicated in Fig. 5(d), the MB adsorption performance decreases as the solution temperature increases. However, when the solution temperature increases from 20 to 45 °C, % of dye adsorption decreases from 87.7% to 70%. This situation was attributed to the fact that when the temperature increases the physical links among the MB particles and the sorbent's vacant sites decrease, resulting in a decrease in the MB adsorption percentage. It was also discovered that MB adsorption onto PC leaves follows exothermic process, as evidenced by the projected trajectory in decreasing the percentage of adsorption efficiency as temperature increased.[32]

3.3. Kinetic study

An understanding of the kinetics of biosorption processes is necessary for the development of decontamination techniques on an industrial scale. To investigate the kinetics of the biosorption process, information from the adsorption data dependent on contact time was utilized. Pseudo-first-order (eqn (1)) and pseudo-second-order (eqn (2)) models were applied to investigate kinetics and to describe the adsorption process. The linear form of the pseudo-first-order (PFO) is given as:

$$\ln(q_e - q_t) = \ln q_e - K_1 t \quad (1)$$

where q_t and q_e are the MB adsorption amounts at time t and at equilibrium, respectively, and K_1 is the rate constant of the PFO adsorption. The adsorption capacity at equilibrium (q_e) was calculated using the intercept of a linear plot of $\ln(q_e - q_t)$ *vs.* t. The R^2 values indicate that the PFO equation could not accurately represent the entire adsorption process.

The linear pseudo-second order (PSO) is given as (eqn (2)):

$$t/q_t = 1/K_2 q_e^2 + 1/q_e t \quad (2)$$

where q_t and q_e are the adsorption amounts at time t and at equilibrium, while K_2 is the PSO rate constant. The slope of the t/q_t *versus* t plot helps to measure the value of q_e, and the

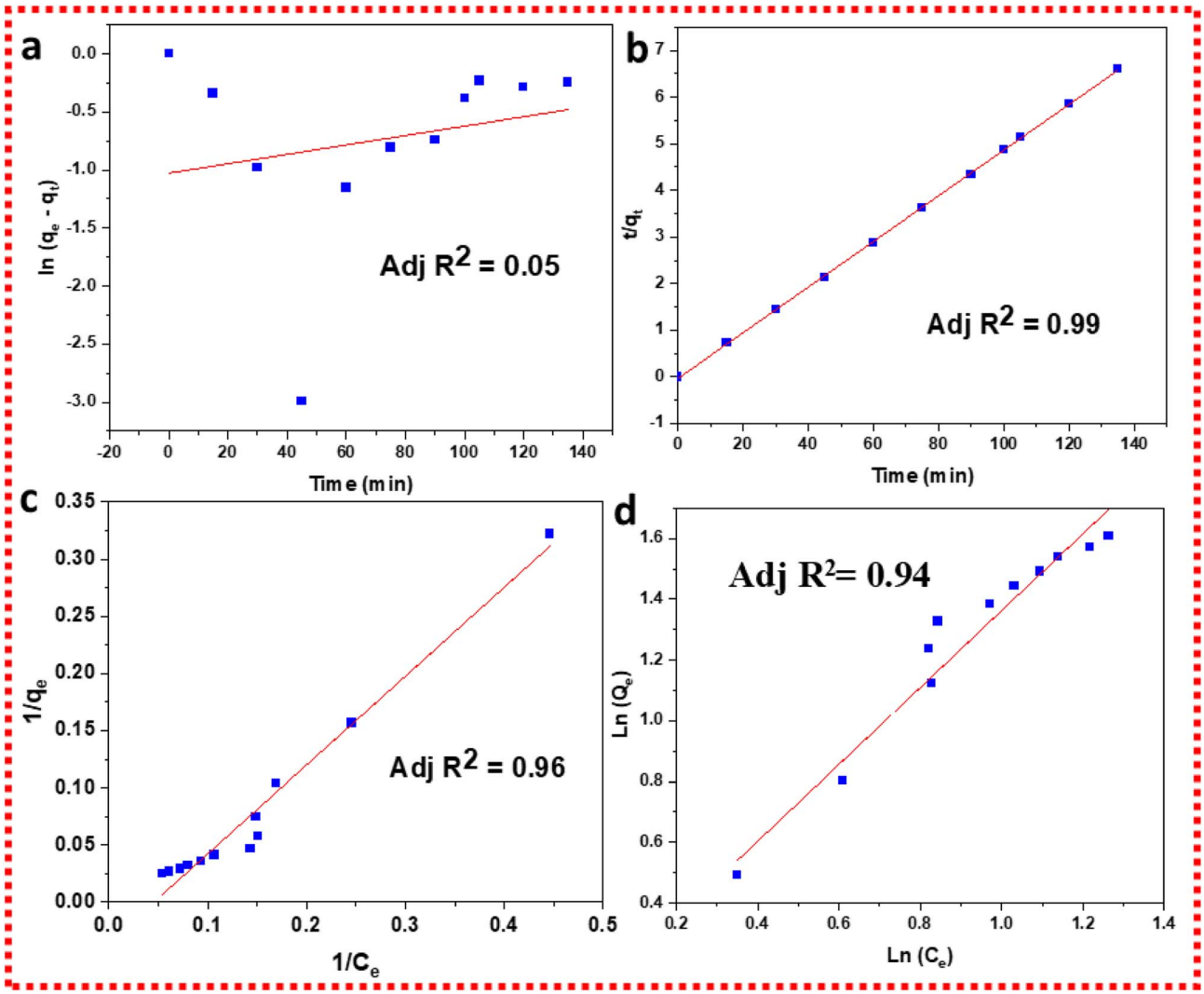

Fig. 6 Pseudo 1st order kinetics (a), pseudo 2nd order kinetics (b), Langmuir adsorption model (c), Freundlich adsorption model (d).

intercept can be employed for the calculation of (K_2). The plot of t/q_t *versus* t yields a straight line. The model's correlation coefficient (R^2) indicates a better fit to adsorption data, and it is 0.9998 (Fig. 6(a and b)).[33]

3.4. Adsorption isotherms

The solid–liquid phase interaction during equilibrium in the adsorption process is mainly determined by the adsorption isotherm. The equation parameters and fundamental thermodynamic concept of isotherm models provide valuable information about the adsorption mechanism, surface characteristics, and affinity in terms of the biosorbent. The two isotherm equations, Langmuir and Freundlich isotherms were used to determine the equilibrium data (Fig. 6(c and d)).

Measurements of absorbance were made both before and after adsorption of MB solutions at $\lambda_{max} = 668$ nm to assess the equilibrium adsorption isotherms of the dye on powdered PC leaves. The equilibrium concentrations (C_e) and the amount of dye adsorbed (q_e) by the biosorbent were determined using the absorbance values.

The Langmuir isotherm describes a monolayer adsorption process on the surface of an adsorbent with a fixed number of sites for adsorbate in aqueous solutions. The linearized equation of Langmuir model can be given as (eqn (3)):

$$1/q_e = 1/q_m + 1/q_m k_L 1/C_e \quad (3)$$

where, q_e (mg g^{-1}) is the quantity of dye adsorbed per unit adsorbent's mass at equilibrium time, C_e (mg L^{-1}) is the dye concentration at equilibrium in the solution, q_{max} (l mg^{-1}) are the Langmuir constants associated with the maximum monolayer adsorption capacity.

The linearized version of Freundlich model can be given as (eqn (4)):

$$\text{Ln } q_e = \ln K_f + 1/n \ln C_e \quad (4)$$

where K_f (l g^{-1}) is the Freundlich constant, showing the capacity of adsorption and n is the Freundlich exponent that shows the intensity of adsorption.

The findings show that biosorbent (PC) adsorbed MB favorably, with high correlation coefficient values ($R^2 = 0.9715$) for Langmuir isotherm (Fig. 6(c)). It suggests that the equilibrium data best fit the Langmuir isotherm, implying monolayer sorption of MB on PC (adsorbent).

Because of its wide availability from local sources and high biosorption intensity for MB, PC leaf powder is a valuable low-cost biosorbent for the economical treatment of MB-contaminated water.[34,35]

3.5. Thermodynamic investigations

To achieve economical and sustainable results, it is important to comprehend the energy characteristics of adsorption ($\Delta G°$, $\Delta H°$, $\Delta S°$), as well as the adsorbent's capacity to renew itself.[36] This study evaluated various thermodynamic parameters of MB adsorption on PC leaf powder at different applied temperatures (298 K) (Fig. 7). The distribution coefficient of adsorption (K_d)

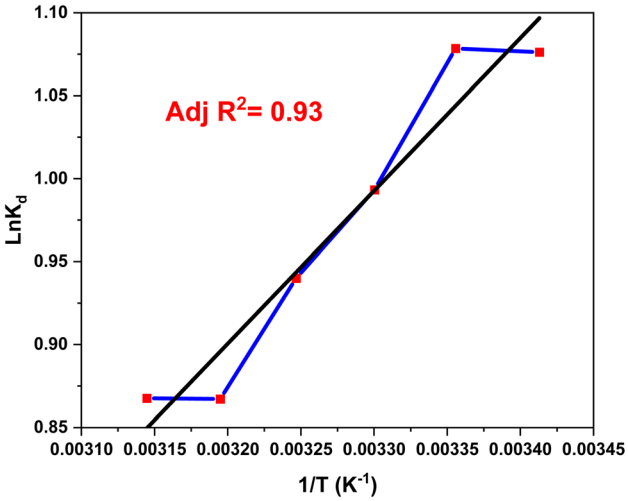

Fig. 7 Thermodynamic parameters for MB adsorption using *Populous ciliata* leaf powder.

was calculated using eqn (5), which connects the concentration of solutes in the aqueous phase (C_{aq}) to the equilibrium concentration (C_e) in mg L^{-1}:

$$K_d = \frac{C_{aq}}{C_e} \quad (5)$$

Applying the Van't Hoff eqn (6), these coefficients help to determine thermodynamic variables including changes in enthalpy (ΔH^*) and entropy shift (ΔS^*).

$$\text{Ln } K_d = \frac{-\Delta H°}{R}\frac{1}{T} + \frac{\Delta S°}{R} \quad (6)$$

The amount of free energy change ($\Delta G°$), enthalpy change ($\Delta H°$), and entropy change ($\Delta S°$) during the adsorption of MB on powdered PC leaves were determined using the following eqn (7) and (8).

$$\Delta G° = -RT \ln K_d \quad (7)$$

$$\Delta G° = \Delta H° - T\Delta S° \quad (8)$$

The thermodynamic study of MB sorption onto PC leaf powder shows that the entire procedure is both spontaneous and exothermic, as shown in Table 1. The negative values for $\Delta G°$ and $\Delta H°$ support these findings. Adsorption reduces randomness at the solid–liquid junction, as indicated by a negative shift in $\Delta S°$. These findings are consistent with prior investigations on plant based biosorbents.[37,38] These observations are supported by the adsorption behavior predicted by the pseudo-second-order model, which reveals a complex interaction of adsorption forces at the interface between MB and PC leaf powder.[32,39]

3.6. Reusability of biosorbent

The stability of PC leaf powder is critical to its practical and long-term use as a biosorbent for adsorption of targets from

Table 1 Calculated thermodynamic parameters; $\Delta G°$, $\Delta H°$ and $\Delta S°$

Sr. no.	Temperature (K)	C_{aq} (mg L^{-1})	C_e (mg L^{-1})	K_d	$\Delta G°$ (kJ mol^{-1})	$\Delta H°$ (kJ mol^{-1})	$\Delta S°$ (kJ mol^{-1} K^{-1})	Adj R^2
1	293	10	3.6	2.77	−2.481914			
2	298	10	3.4	2.94	−2.671837			
3	303	10	3.7	2.70	−2.502142	−7.6	−17	0.93
4	308	10	3.9	2.56	−2.407088			
5	313	10	4.2	2.38	−2.25644			
6	318	10	4.7	2.12	1.986633			

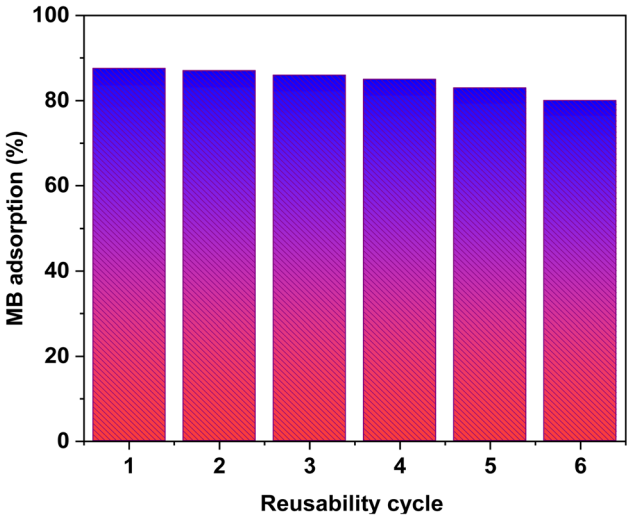

Fig. 8 Reusability of biosorbent for MB adsorption.

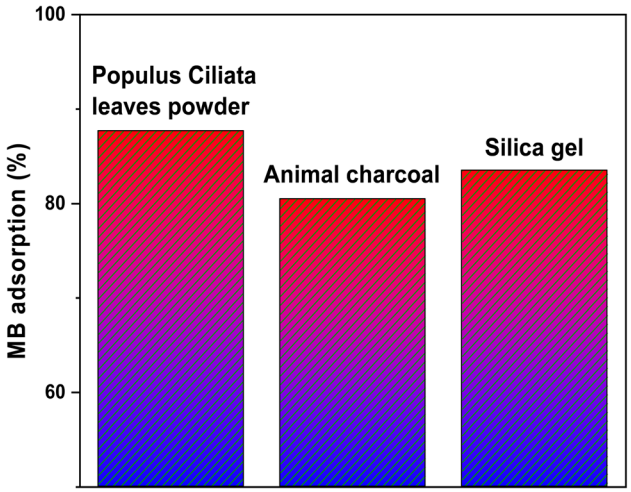

Fig. 9 Comparison of % adsorption of PC leaves with silica gel and animal charcoal for adsorption of MB.

aqueous solutions. The stability of PC leaf powder was investigated by recycling the biosorbent for MB adsorption six times, with the results given in Fig. 8. Each of the cycle of MB adsorption was investigated for 45 min using 60 mg biosorbent and 10 mg MB at pH 7. After every adsorption cycle, the PC leaf powder (biosorbent) was collected by centrifugation, rinsed with deionized water, and dried for reuse. After six cycles, the MB adsorption efficiency dropped marginally from 87.7% to 80%. Recycling the biosorbent for MB adsorption many times indicated that the surfaces of the biosorbent were largely intact and resilient, with a minor drop in adsorption efficiency. Furthermore, MB was not permanently incorporated on the surface of PC leaf powder, therefore the biosorbent was readily removed from the pollutant using centrifugation. A modest drop in efficiency with the subsequent use of biosorbent was assumed to be related to the blocking some of the active sites prevalent on the surfaces of the biosorbent 2.

3.7. Comparison of adsorption efficiency of *Populus ciliata* leaf powder with the commercially employed adsorbents

The purpose of this study was to evaluate the effectiveness of PC leaf powder-based biosorbent relative to widely employed adsorbents like animal charcoal and silica gel. For this purpose, 100 mL of 10 mg per L MB solution at pH 7 was taken in three 200 mL beakers. Their absorbance values were noted using a UV/vis spectrophotometer. In these solutions, 60 mg adsorbent doses of animal charcoal, silica gel, and PC leaf powder were added and then shaken on a digital orbital shaker for the ideal amount of time to achieve MB equilibrium on the adsorbent. The dye solutions were filtered and examined for absorbance measurement once adsorption equilibrium was reached. It was noted that PC leaf powder exhibited slightly better dye adsorption capacity compared to silica gel and animal charcoal. Animal charcoal and silica gel adsorbed 80.57% and 83.59% of the MB, respectively, while PC leaf powder adsorbed 87.70% of the dye (Fig. 9). Slight variation in adsorption performance of PC leaf powder, animal charcoal, and silica gel may be attributed to nature and availability of active sites persisting on the surface of these adsorbents. These results support the successful application of PC leaf powder for MB adsorption from aqueous samples.

3.8. Comparison of the *Populus ciliata* leaf powder's adsorption properties to the previously reported adsorbents

To confirm the viability of synthesized PC leaf powder for MB adsorption, the adsorption capacity of the synthesized biosorbent was compared with other biosorbents like almond shells, cellulose-based adsorbents, and peanut husk. As

Table 2 Comparison of adsorption capacity of *Populus ciliata* leaf powder with reported low-cost adsorbents

No.	Adsorbents	Adsorption time (min)	Adsorbent amount (mg)	MB concentration ($mg\ L^{-1}$)	pH	Temperature (K)	Partition coefficient ($mg\ g^{-1}\ \mu M^{-1}$)	q_e ($mg\ g^{-1}$)	References
1	Neem leaf powder	300	2000	40	7	300	3.11	19.61	41
2	Banana leaf powder	20	1000	100	7.2	303	2.91	15.9	42
3	*Mangifera indica* leaf powder	60	10	100	7	303	2.61	6.6	43
4	Fig leaf-activated carbon	60	80	80	7	298	4.13	24.7	44
5	Dried uncharred leaves of *Ficus benjamina*	5760	2000	100	6	298	3.69	25.4	45
6	*Populus ciliata* leaf powder	45	60	10	7	298	4.39	22.098	Current study

indicated by Table 2, PC leaf powder showed comparable adsorption capacity with the previously reported biosorbents. Additionally, the comparative study for MB adsorption revealed that PC leaf powder had the greatest partition coefficient and rate constant among all adsorbents (Table 2). Elevated partition value demonstrates the excellent affinity of the PC surface functional groups for MB molecules, demonstrating effective dye separation from the liquid phase to the solid layer. The increased rate constant also indicates quick adsorption equilibrium due to plentiful active binding sites, substantial surface reactivity, and an abundance of oxygen- and nitrogen-containing functional structures that facilitate electrostatic and π–π interactions. These parameters indicate that PC leaf powder has quicker adsorption kinetics and higher dye-binding effectiveness than other plant-based adsorbents.[40] From the robust performance of PC leaf powder, it was anticipated that it holds significant implications for environmental applications, providing a sustainable solution for mitigating the detrimental effects of dye pollution in wastewater.

4. Conclusion

The study demonstrates the potential of *Populus ciliata* (PC) leaf powder as a highly efficient biosorbent for the adsorption of a cationic dye (MB) from aqueous solutions. The remarkable adsorption capabilities of this natural material hold promise for addressing the pressing issue of dye pollution in various contexts. In essence, the study employed a cost-effective and environment friendly approach to produce the PC leaf powder as biosorbent. To ascertain its suitability, the biosorbent underwent comprehensive characterization techniques such as FTIR, BET, SEM, and EDX, confirming the presence of crucial features like morphological attributes, elemental composition, and functional groups that are essential for effective dye adsorption. Subsequently, a series of batch adsorption experiments were conducted systematically by varying experimental parameters including contact time, adsorbent dosage, pH, ionic strength, and initial dye concentration.

The observed adsorption kinetics revealed a notable fit with the pseudo-second-order model, supported by high R^2 values, indicating the occurrence of chemisorption. Moreover, the Langmuir model well described the adsorption behavior, indicating a monolayer adsorption process on a homogeneous surface. Additionally, the adsorbent performed exceptionally well in various salinity conditions as well as in river and tap water, allowing for direct commercial-level use without any kind of treatment to adsorb tainting dyes from wastewater used in industry.

The remarkable adsorption ability of PC leaf powder for methylene blue implies that it might be used as a cost-effective, environmentally acceptable biosorbent in wastewater treatment processes. Future research might concentrate on improving adsorption conditions and developing the technique for commercial applications. Furthermore, manipulating the PC leaf powder with chemical or thermal processes may improve its adsorption effectiveness and recyclability. Investigating its

efficiency against more organic effluents and heavy metals may widen its application for ecological remediation.

Conflicts of interest

The authors declare that they have no financial or personal interests.

Data availability

The authors confirm that the data supporting the findings of this study are available within the article.

Acknowledgements

This work was supported and funded by the Deanship of Scientific Research at Imam Mohammad Ibn Saud Islamic University (IMSIU) (grant number IMSIU-DDRSP2502).

References

1 S. Rani, P. Kumar and N. Kataria, *J. Taiwan Inst. Chem. Eng.*, 2025, **166**, 105566.
2 K. Aziz, A. Naz, S. Manzoor, M. I. Khan, A. Shanableh and J. Fernandez Garcia, *Catalysts*, 2023, **13**, 1087.
3 A. E. Alprol, M. A. El-Sheikh, P. Pereira and H. M. Khairy, *Biomass Convers. Biorefin.*, 2025, 1–20.
4 K. Aziz, A. Naz, N. Raza, S. Manzoor and K.-H. Kim, *Environ. Res.*, 2024, **247**, 118256.
5 S. P. Alzura, V. Saraswaty, S. Ishmayana, Y. P. Budiman, D. R. Eddy, E. S. Aji, D. Ratnaningrum, E. S. Endah, H. Meirinawati and H. Setiyanto, *Case Stud. Chem. Environ. Eng.*, 2025, **11**, 101113.
6 N. Kanwal, K. Aziz, A. Naz, N. Raza, Z. Ali, M. Khairy, A. Azzouz and A. A. Chaudhary, *Diamond Relat. Mater.*, 2025, 112553.
7 M. Akhtar, M. Sarfraz, M. Ahmad, N. Raza and L. Zhang, *Desalin. Water Treat.*, 2025, **321**, 100914.
8 G. Tejaswini, S. Beebi and V. D. Praveena, *Polyhedron*, 2025, **274**, 117500.
9 A. M. Shabbirahmed, A. Jacob, P. Dey, P. Somu and D. Haldar, *Discover Appl. Sci.*, 2025, **7**, 771.
10 A. H. Gharbi, H. Hemmami, S. E. Laouini, I. B. Amor, S. Zeghoud, A. B. Amor, F. Alharthi, A. Barhoum and J. A. A. Abdullah, *Biomass Convers. Biorefin.*, 2025, **15**, 701–712.
11 A. K. Tolkou, E. K. Tsoutsa, G. Z. Kyzas and I. A. Katsoyiannis, *Environ. Sci. Pollut. Res.*, 2024, **31**, 14662–14689.
12 N. S. Sayed, A. S. Ahmed, M. H. Abdallah and G. A. Gouda, *Sci. Rep.*, 2024, **14**, 5384.
13 K. Ngiwngam, P. Rachtanapun, G. Kasi, J. Han and W. Tongdeesoontorn, *Bioresour. Technol. Rep.*, 2024, **27**, 101955.
14 M. Aliannezhadi, F. Doost Mohamadi, M. Jamali and F. Shariatmadar Tehrani, *Sci. Rep.*, 2025, **15**, 7203.
15 D. Purushotham, A. Mavinakere Ramesh, D. Shetty Thimmappa, N. Kalegowda, G. Hittanahallikoppal Gajendramurthy, S. P. Kollur and M. Mahadevamurthy, *Int. J. Mol. Sci.*, 2025, **26**, 4739.
16 M. Hafeeza, R. Shaheena, S. Alib, H. Shakirc, M. Irfand, T. Mughalb, A. Hassanb, M. Khane and S. Mumtazb, *Dig. J. Nanomater. Biostruct.*, 2021, **16**, 899–906.
17 A. Sekar, P. JothiMurugan, G. Shanmugam, B. Gassoumi, M. M. Al-Ansari, P. Srinivasan, S. Nivetha, F. Paularokiadoss and S. Ayachi, *Luminescence*, 2025, **40**, e70158.
18 M. Hafeez, M. Zeb, A. Khan, B. Akram, Z. u. Abdin, S. Haq, M. Zaheer and S. Ali, *Microsc. Res. Tech.*, 2021, **84**, 480–488.
19 M. Hafeez, R. Arshad, J. Khan, B. Akram, M. N. Ahmad, M. U. Hameed and S. Haq, *Mater. Res. Express*, 2019, **6**, 055043.
20 S. Malik, G. Kumaraguru, M. Bruat, F. Chefdor, C. Depierreux, F. Héricourt, S. Carpin, G. Shanmugam and F. Lamblin, *Protoplasma*, 2024, **261**, 1311–1326.
21 H. Shukor, A. Z. Yaser, N. F. Shoparwe, M. Mohd Zaini Makhtar and N. Mokhtar, *Int. J. Chem. Eng.*, 2022, **2022**, 8153617.
22 M. Hafeez, R. Shaheen, B. Akram, S. Haq, S. Mahsud, S. Ali and R. T. Khan, *Mater. Res. Express*, 2020, **7**, 025019.
23 J. W. Osterrieth, J. Rampersad, D. Madden, N. Rampal, L. Skoric, B. Connolly, M. D. Allendorf, V. Stavila, J. L. Snider and R. Ameloot, *Adv. Mater.*, 2022, **34**, 2201502.
24 S. Saghir, C. Pu, E. Fu, Y. Wang and Z. Xiao, *Surf. Interfaces*, 2022, **34**, 102357.
25 S. Yarik, F. Barka Bouaifel, N. Bezzi, I. Akkari, S. Kessi and K. Bouaouina, *Environ. Monit. Assess.*, 2025, **197**, 768.
26 M. MuthuKathija, S. Muthusamy, R. I. Khan, M. S. M. Badhusha, K. Rajalakshmi, V. Rama and Y. Xu, *Inorg. Chem. Commun.*, 2024, **161**, 111929.
27 A. Boulett, K. Roa, G. Pizarro and J. Sanchez, *Colloids Surf., A*, 2024, **702**, 135055.
28 S. Gul, S. Afsar, N. Raza, H. Gul, L. Khezami, R. Almufarij and S. N. Hussain, *Biomass Convers. Biorefin.*, 2024, **14**, 31079–31092.
29 A. Hedfi, M. Ben Ali, S. Haq, J. Razzokov, W. Rehman, M. Waseem, K. Elmnasri, M. Khalid Hossain, F. U. Rehman and E. Karimbaev, *Open Chem.*, 2025, **23**, 20250132.
30 P. Elango, S. Ramar, A. Gurusamy, B. Muthukutty, P. Jeganathan and M. Sivakumar, *Colloids Surf., A*, 2025, **709**, 136147.
31 S. Abbas, T. Javeed, S. Zafar, M. B. Taj, A. R. Ashraf and M. I. Din, *Desalin. Water Treat.*, 2021, **233**, 387–398.
32 S. Gul, N. Raza, S. Gul, H. Gul, S. Afridi, L. Khezami, M. A. Habib, A. Hajjaji and A. Azzouz, *Water, Air, Soil Pollut.*, 2025, **236**, 615.
33 S. Yetgin and M. Amlani, *Clean Technol. Environ. Policy*, 2025, **27**, 1205–1225.
34 A. Doi, M. Ganguly and M. Sahu, *Adsorption*, 2024, **30**, 1603–1630.
35 B. Alouche, A. Dehbi, S. Bassaid, A. Yahiaoui, A. Alsalme and M. Messori, *React. Kinet., Mech. Catal.*, 2025, **138**, 1535–1552.

36 A. M. Scott, L. Gorb, E. A. Burns, S. N. Yashkin, F. C. Hill and J. Leszczynski, *J. Phys. Chem. C*, 2014, **118**, 4774–4783.
37 C. R. Girish, *Chem. Pap.*, 2025, 1–20.
38 M. N. Sahmoune, *Environ. Chem. Lett.*, 2019, **17**, 697–704.
39 S. Gul, S. Gul, H. Gul, N. Raza, A. Azzouz, M. R. Elamin and L. Khezami, *Biomass Convers. Biorefin.*, 2025, **15**, 4225–4241.
40 A. Strebel, M. Behringer, H. Hilbig, A. Machner and B. Helmreich, *Front. Environ. Eng.*, 2024, **3**, 1347981.
41 K. G. Bhattacharyya and A. Sharma, *Dyes Pigm.*, 2005, **65**, 51–59.
42 G. Annadurai, R.-S. Juang and D.-J. Lee, *J. Hazard. Mater.*, 2002, **92**, 263–274.
43 D. N. Shetty, V. A. Lobo, S. Rani and N. Raghavendra, *Hybrid Adv.*, 2024, **7**, 100316.
44 S. T. Al-Asadi, F. F. Al-Qaim, H. F. S. Al-Saedi, I. F. Deyab, H. Kamyab and S. Chelliapan, *Environ. Monit. Assess.*, 2023, **195**, 676.
45 V. Watwe, S. Kulkarni and P. Kulkarni, *Ind. Crops Prod.*, 2023, **195**, 116449.